Surface Self-Diffusion of Organic Molecules Adsorbed in Porous Silicon

Rustem Valiullin,*,†,‡ Pavel Kortunov,‡ Jörg Kärger,‡ and Viktor Timoshenko§

Department of Molecular Physics, Kazan State University, Kazan 420008, Russia, Abteilung Grenzflaschephysik, Universität Leipzig, Linnestr. 5, Leipzig 04103, Germany, and Physics Department, Moscow State University, Moscow 119992, Russia

Received: September 21, 2004; In Final Form: January 24, 2005

The pulsed field gradient nuclear magnetic resonance method has been employed to probe self-diffusion of organic guest molecules adsorbed in porous silicon with a 3.6 nm pore size. The molecular self-diffusion coefficient and intrapore adsorption were simultaneously measured as a function of the external vapor pressure. The latter was varied in a broad range to provide pore loading from less than monolayer surface coverage to full pore saturation. The measured diffusivities are found to be well-correlated with the adsorption isotherms. At low molecular concentrations in the pores, corresponding to surface coverages of less than one monolayer, the self-diffusion coefficient strongly increases with increasing concentration. This observation is attributed to the occurrence of activated diffusion on a heterogeneous surface. Additional experiments in a broad temperature range and using binary mixtures confirm this hypothesis.

Introduction

The knowledge of dynamic properties of adsorbed molecules in pores is one of the crucial factors determining the success of surface chemistry in modeling chemical reactions in porous catalysts. Adsorbate diffusion is, in many cases, a key parameter controlling the efficiency of catalytic reactions. The relevance of diffusion phenomena concern both the microscopic scale, where they determine the local reaction rates, and the macroscopic scale, by governing the rates of reactant supply and product removal. Thus, the understanding of how details of a porous structure and surface characteristics are interrelated with the adsorbate dynamics is of importance for many industrial processes where porous catalysts play a central role. It is well-recognized that surface diffusion, i.e., molecular displacements along the pore surface, is one of the most important modes of molecular dynamics in pores, especially at low pore loadings. Moreover, due to their enormous specific surface, nanoporous materials attain increasing significance in modern science, leading to an additional reinforcement of the interest in surface diffusion phenomena. Finally, as another important aspect, diffusion studies may provide additional valuable information for surface characterization. Reconstruction of energetic properties from adsorption properties does not always provide a satisfactory result.[1,2] It was pointed out that a joint analysis of adsorption and diffusion data may represent a most helpful, complementary data set for elucidating the surface properties.[3]

Experimental studies of surface diffusion in various adsorbate−adsorbent systems have been widely reported and reviewed in the literature.[4−6] However, they are mostly concerned with the transport (or chemical) diffusion coefficient, which interrelates concentration gradients with resulting fluxes and which, therefore, is obtained under nonequilibrium conditions. The process of self-diffusion, which proceeds via molecular hopping between adjacent surface sites under equilibrium conditions, is considered to a lesser extent. Recent progress in the development of experimental techniques, such as scanning tunneling microscopy and field ion microscopy, allowed the tracking of single molecules on surfaces and led to a revision of such phenomena in surface self-diffusion as identification of double jumps on the surface or diffusion of clusters, e.g., dimers or trimers.[7−9] It should be noted that the applicability of these techniques is limited to very short time scales and low surface coverages.

Pulsed field gradient nuclear magnetic resonance (PFG NMR) is a powerful noninvasive method, which has been successfully used to probe the details of molecular self-diffusion in many porous materials.[10−12] This method is based on the creation of an initial nuclear coherence and following its loss due to the molecular displacements in an applied magnetic field gradient. Thus, the characteristics of molecular motion under equilibrium conditions may be followed in a broad time scale from milliseconds to seconds. Alternatively, a similar method relying on intrinsic magnetic field gradients has been successfully used to gain information about the adsorbate state in pores, which, in turn, may be used to probe molecular diffusion.[13] Some attempts to probe surface diffusion using the PFG NMR method have been made earlier, exploiting samples with different pore-filling factors[14−17] or surface-induced liquid layers formed upon freezing.[18] However, in all these studies the partial surface coverages, or pore fillings corresponding to less than monolayer coverage, were not systematically covered. In the present paper, we apply the PFG NMR method to investigate the self-diffusion of organic molecules, cyclohexane and acetone, physisorbed in porous silicon with a small pore diameter of about 3.6 nm. The experimental setup allowed us to measure simultaneously self-diffusion and intrapore adsorption as a function of the external vapor pressure. The latter was varied over a broad range, providing pore loadings from less than a monolayer surface coverage to full pore saturation.

Experimental Section

Materials. Porous silicon[19,20] (PSi) was prepared by electrochemical etching (anodization) of single-crystalline (100)-

* Author to whom correspondence should be addressed. Phone: (49) 0341 97 32 515. Fax: (49) 0341 97 32 549. E-mail: valiulli@rz.uni-leipzig.de.

† Kazan State University.

‡ Universität Leipzig.

§ Moscow State University.

10.1021/jp045721p CCC: $30.25
Published on Web 02/25/2005

oriented p-type Si wafers (of about 3 cm diameter and 120 μm thickness) with resistivity of 10 Ω cm. The electrolyte contained HF (50%) and C_2H_5OH in a ratio of 2:1. The anodization current density was 30 mA/cm^2, and the anodization time was 75 min. For removing the porous silicon film from the substrates, we applied an electropolishing step with a current density of 500 mA/cm^2 for 2−3 s. The prepared porous silicon wafers were crushed to small pieces (of about 1−2 mm length) for subsequent use. The liquids under study, acetone, cyclohexane, and nitrobenzene, were purchased from Merck (Merck, Germany) and used without further purification.

Characterization of Porous Silicon. According to the literature data, the described preparation procedure yields a mean pore diameter of the prepared PSi of about 2−3 nm.[20] Moreover, the pores are expected to be separated from each other and of close to cylindrical in their morphology.[21,22] To determine a pore-size distribution of the PSi under study, the NMR version[23] of thermoporometry has been employed. This method utilizes the fact that the melting temperature $T_m(d)$ for frozen liquids in a pore with diameter d is suppressed with respect to the value T_m in the bulk phase, following the Gibbs−Thompson relation

$$T_m - T_m(d) = \frac{4\gamma_{sl}\upsilon_s}{d\Delta H_{sl}} \equiv \frac{K}{d} \quad (1)$$

where γ_{sl} is the surface energy of the solid phase, υ_s is the molar volume, and ΔH_{sl} is the solid−liquid transition enthalpy. In a liquid-saturated sample, for sufficiently low temperatures the frozen liquid will assume the shape of the porous space. Upon warming, melting of the intraporous phase will occur according to eq 1. This process may be followed by the NMR technique and used to derive the pore-size distribution function $f(d)$. Indeed, NMR signals from the crystal and liquid phases are easily distinguished due to the large difference in their spin−spin relaxation times. Thus, measuring the liquid NMR signal $I(T)$ as a function of temperature T, one can derive the pore-size distribution function $f(d)$ relying on eq 1 (see ref 23, for details)

$$f(d) = \frac{\partial I(T)}{\partial T}\frac{K}{d^2} \quad (2)$$

The NMR cryoporometry experiments have been carried out on a home-built NMR spectrometer operating at a proton resonance frequency of 400 MHz and equipped with a temperature controller with an accuracy of better than 0.2 K. As a probe liquid, nitrobenzene (T_m = 278.9 K, K = 125 K nm[24]) was used. The activated PSi crystals placed in the NMR tube were oversaturated with nitrobenzene. The ^{1}H NMR measurements were performed using the 90°−τ−180° spin−echo pulse sequence with τ = 3 ms. In this way, due to its short transverse relaxation times, the signal from the crystalline phase could be suppressed. Initially, the sample was cooled to 173 K where almost no liquid signal has been detected. Thereafter, the temperature was increased in steps of 1 K, given 5 min for equilibration, and the intensity of the spin−echo signal was recorded. The procedure was repeated up to 283 K, and the obtained function $I(T)$ is shown in Figure 1a.

The two distinct regions $T \approx 210-260$ K and $T \approx 279$ K in Figure 1a correspond to the melting of intraporous nitrobenzene and of nitrobenzene between the PSi wafers, respectively. The resulting pore-size distribution $f(d)$ obtained using eqs 1 and 2 with the parameters T_m = 278.9 K and K = 125 K nm is shown in Figure 1b. The determined distribution function $f(d)$ is found to have a narrow distribution and asymmetric shape with a mean

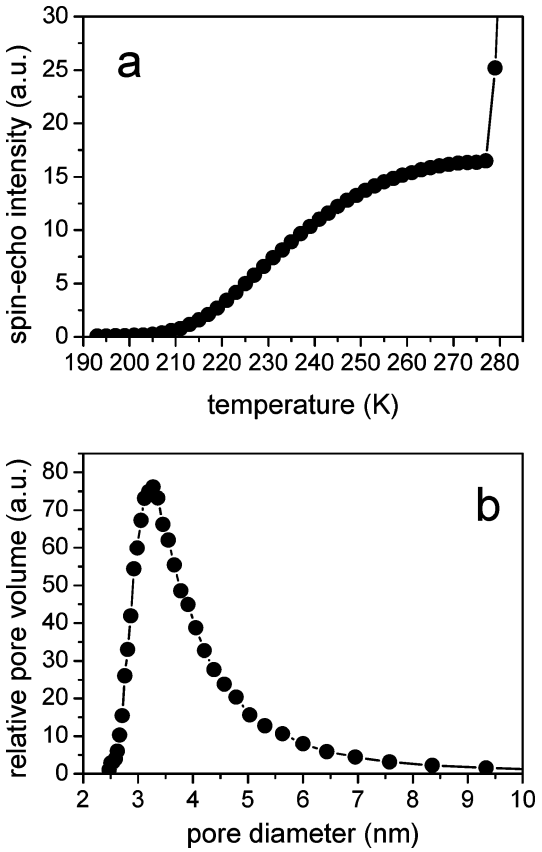

Figure 1. (a) NMR spin−echo intensity I of liquid nitrobenzene in porous silicon as a function of the increasing temperature. (b) The pore-size distribution function $f(d)$ obtained from the data in part a using eq 2. The solid lines are shown as guidelines.

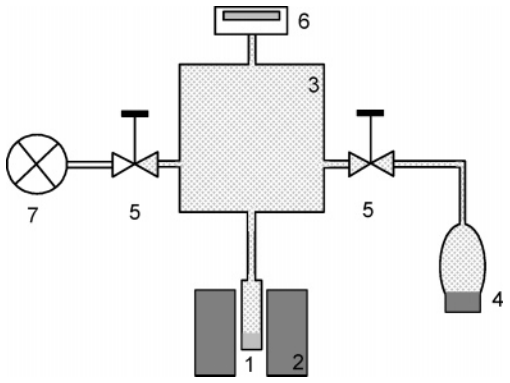

Figure 2. Experimental setup. (1) NMR tube with porous silicon crystals, (2) NMR spectrometer, (3) buffer reservoir; (4) flask with the liquid under study; (5) valves; (6) pressure detector; (7) turbo-molecular pump.

pore diameter $d \approx 3.6$ nm. As a possible reason for the distribution asymmetry, we consider the lowering of the real HF concentration inside a thick PSi layer during the etching process since the pore size is known to increase with decreasing HF content in the solution.[20]

Variation of the Pore Loading. To vary the concentration of liquids in pores, the experimental setup shown in Figure 2 was used. First, a certain vapor pressure was prepared in the buffer reservoir with a much larger volume than that of the total pore volume of the sample. Thereafter, when the interconnecting valve was opened, the sample pressure was equilibrated with that of the buffer volume. The equilibration was followed by recording the signal intensity S_{FID} of the ^{1}H free induction decay (FID). It reflects the total amount of protons and, consequently,

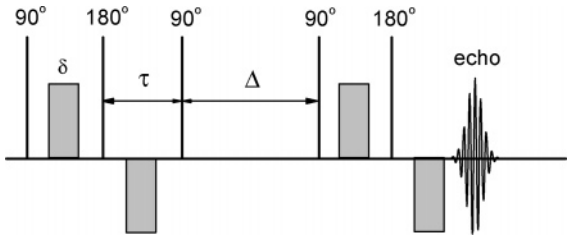

Figure 3. The 13-interval stimulated-echo−pulse sequence. The filled rectangles represent gradient pulses with length δ and amplitude G. The total diffusion time t_d in the notation used is $t_d = \Delta + 3\tau/2 - \delta/6$.

of adsorbed molecules in the sample. The relative adsorbate concentration θ in the pores at a certain vapor pressure was obtained by normalization of the respective S_{FID} with respect to that at full pore saturation. The latter situation corresponds to equilibrium with the saturated vapor.

It is worth noting that the shortened T_2 relaxation times of adsorbate molecules in porous materials with a high specific surface may lead to an improper determination of the FID signal intensity due to a finite dead time t_{dead} of the NMR spectrometer ($t_{dead} = 20$ μs in our case). Therefore, measurements of T_2 relaxation times using the CPMG pulse sequence have been additionally performed. The obtained relaxation times were found to depend on the vapor pressure or, respectively, the pore filling. The shape of the concentration dependence of T_2 followed that of the isotherm with magnitudes varying from $T_2 \approx 150$ ms at full pore saturation to $T_2 \approx 5$ ms at the lowest concentrations attained in the present study for both liquids considered. Most importantly, the condition $T_2 \gg t_{dead}$ was always fulfilled, yielding that any disturbing effect on the determination of the signal intensity as introduced by the spin−spin relaxation is negligible.

PFG NMR Experiments. Simultaneously with the measurement of the adsorption isotherm, the PFG NMR experiments have been carried out. The NMR spectrometer was equipped with a home-built pulsed field gradient NMR unit producing a maximal z-gradient strength ~35 T/m in a 7 mm o.d. NMR sample. For the diffusion measurements, the 13-interval stimulated-echo−pulse sequence (Figure 3) has been applied.[25] The use of this pulse sequence has two advantages: the effect of internal magnetic field inhomogeneities in a sample can be sufficiently reduced and the use of gradients of opposite polarity reduces unwanted eddy current effects.[26,27] The typical parameters of the pulse sequence used in the present study were: $\tau = 600$ μs, $\delta = 400$ μs, and $\Delta = 9.2$ ms. The signal accumulation was performed with the repetition time $\sim 5T_1$, where T_1 was about 1 s for all pore fillings.

For nuclei characterized by a single self-diffusion coeffcient, D, the echo amplitude A is a function of the wavenumber $q = \gamma\delta G$ (γ is the nuclear gyromagnetic ratio, G is the gradient strength) and the effective diffusion time t_d

$$A(q,t_d) = A(0,t_d)\exp\left\{-\frac{4\tau}{T_2} - \frac{\Delta}{T_1}\right\}\exp\{-q^2Dt_d\} \quad (3)$$

where the signal loss due to spin−spin (T_2) and spin−lattice (T_1) relaxations is taken into account. Usually, during the experiments the times Δ and τ are kept constant, and only the gradient strength G is varied. In this case, the normalized spin−echo attenuation

$$S(q,t_d) = A(q,t_d)/A(0,t_d)\exp\left\{-\frac{4\tau}{T_2} - \frac{\Delta}{T_1}\right\} = \exp\{-q^2Dt_d\} \quad (4)$$

is determined by only the diffusion term.

If the diffusion process takes place in a restricted geometry, i.e., in pores of a given morphology, then it may lead to a deviation of the spin−echo attenuation shape from that given by eq 4. This is, indeed, the case in the present study. The sample consists of the porous silicon chips with straight nonintersecting channels perpendicular to their surface so that long-range molecular diffusion can only proceed along these channels.[10,28] In general, with the distribution function $F(\phi)$ describing an orientation probability of the tube axes with respect to the magnetic field gradient direction, $S(q,t_d)$ is given by

$$S(q,t_d) = \int_0^\pi F(\phi)\exp\{-q^2Dt_d\cos^2(\phi)\}\sin(\phi)\,d\phi \Big/ \int_0^\pi F(\phi)\sin(\phi)\,d\phi \quad (5)$$

Because the thickness of the porous silicon chips (~120 μm) obtained upon crushing is much less than their mean length (~1 mm), orientation of the wafers in the NMR tube cannot be assumed to be isotropic. Rather, one has to expect a preferential chip orientation parallel to the tube bottom. To take this into account, we have modeled the orientation function $F(\phi)$ using a normal distribution

$$F(\phi) = \frac{1}{\sqrt{2\pi}\omega}\exp\left\{-\frac{(\cos(\phi)-1)^2}{2\omega^2}\right\} \quad (6)$$

of the channel orientation around the sample axis and hence the direction of the field gradient ($\phi = 0$). The diffusivities were obtained by fitting eq 5 with $F(\phi)$ given by eq 6 to the experimental data. It should be noted that in case of the nonexponential spin−echo attenuation functions the effective diffusivities are often determined by fitting eq 4 to the initial part of $S(q,t_d)$. With respect to the diffusion process within channels, such fitting results in an apparent diffusivity

$$D_{app} = D\int_0^\pi F(\phi)\cos^2(\phi)\sin(\phi)\,d\phi \Big/ \int_0^\pi F(\phi)\sin(\phi)\,d\phi \quad (7)$$

i.e., depending on the shape of $F(\phi)$ D_{app} deviates from the true diffusivity D by a numerical factor ranging from $^1/_3$ for isotropic distribution to 1 for orientation of channels parallel to the magnetic field gradient. The approach based on the use of eq 5 with $F(\phi)$ modeled by some analytical function (e.g., in the form of eq 6) allows exclusion, at least partial, of this numerical factor. It is also important to note that in the present study we are primarily interested in dependencies of the molecular diffusivities in the pores on the vapor pressure P. Under the reasonable assumption that the orientation function $F(\phi)$ does not change with saturation of the porous silicon chips by the liquid (recall that the saturation is related to P), one can fit the data, keeping the parameter ω in eq 6 constant over the entire range of the vapor pressures. This means that a possible deviation of $F(\phi)$ modeled by eq 6 from the real one existing in the sample will only slightly shift the whole function $D(P)$ up or down, affecting in no way its shape.

Experimental Results and Discussion

In Figure 4, the experimentally obtained concentrations θ of the adsorbate molecules and their diffusivities D in the porous silicon are shown as a function of the relative pressures $z = P/P_s$ at $T = 297$ K. The saturated vapor pressures P_s for acetone and cyclohexane at this temperature are 29.3×10^3 and 12.4×10^3 N/m^2, respectively. In this paper, we confine ourselves to presenting the results obtained on desorption. Because of the

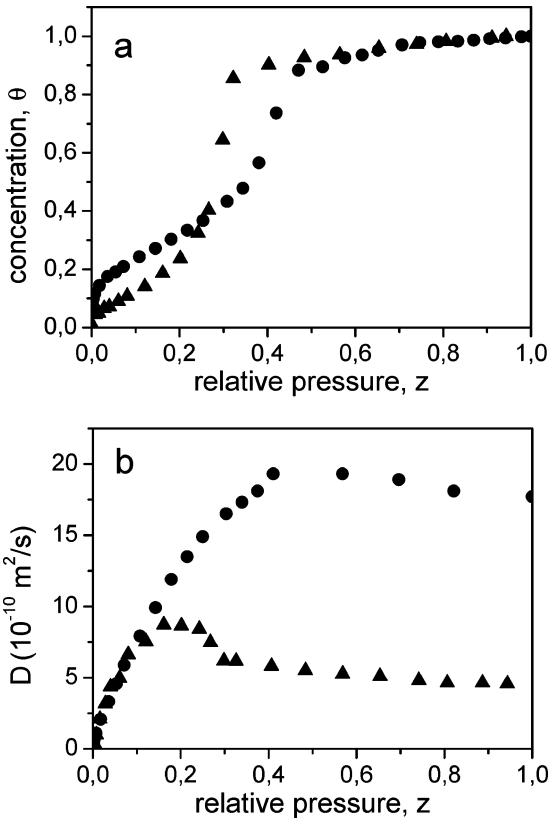

Figure 4. (a) Concentration θ of molecules and (b) the self-diffusion coefficient D for cyclohexane (triangles) and acetone (circles) in porous silicon as a function of the relative pressure z. D were obtained by fitting eq 5 with eq 6 to the measured echo attenuations $S(q,t_d)$. The best fit yielded $\omega \approx 0.3$ for all relative pressures and both liquids under study.

usually observed hysteresis in adsorption−desorption isotherms, the experimental data on the adsorption branch were found to be slightly different from those on the desorption branch. In the present study, however, this difference is of minor relevance. It is seen from Figure 4 that the dependencies of the obtained self-diffusion coefficients on the vapor pressure are interrelated with the shape of the isotherms. At relatively high pressures, the diffusivities are nearly constant, corresponding to the existence of a phase of capillary condensation in the pores. The latter is reflected by the high-pressure shoulder of the isotherms. When, with decreasing pressure, the liquid meniscus breaks at a certain pressure value, the self-diffusion coefficient either passes a maximum (cyclohexane) or decreases (acetone) with further decreasing pressure. In this pressure range, two phases coexist with each other: a phase adsorbed on the pore walls and the gaseous phase in the pore interior. In the following, we are going to estimate the contributions of these two molecular ensembles to a measured diffusivity D.

With the observation time $t_d = 10$ ms used in this study and with the diffusivity data of Figure 4b, the molecular mean displacements $r \propto \sqrt{Dt_d}$ are estimated to be longer than 1 μm for the whole range of vapor pressures considered. Importantly, these displacements significantly exceed the channel diameters, while they are negligibly small in comparison with the channel length. Thus, over the total experiments, molecular diffusion can be assumed to be ideally one-dimensional, leading to a Gaussian propagation pattern.[11] We have carefully checked that variation of the observation time from 4 to 100 ms does not lead to any change of the measured spin−echo attenuation functions and, consequently, of the measured diffusivities D, within the experimental precision. This confirms the Gaussian

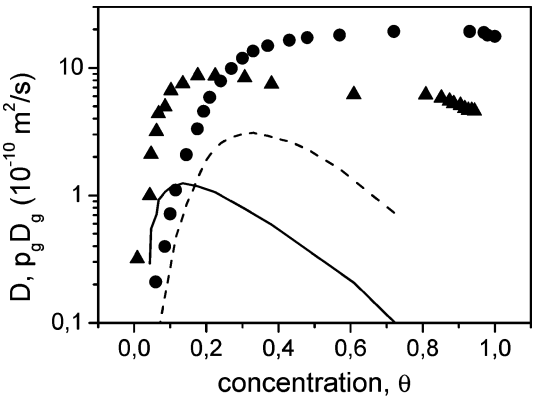

Figure 5. Concentration dependencies of the self-diffusion coefficients D (experimental data, redrawn from Figure 4b) for cyclohexane (triangles) and acetone (circles) and of the term p_gD_g (calculated using eq 9 with $z(\theta)$ taken from Figure 4a) for cyclohexane (solid line) and acetone (dashed line) in porous silicon.

character of the self-diffusion process in the given scale. Thus, we conclude that during t_d the molecules experience many cycles consisting of displacements along the surface, desorption, and subsequent adsorption after performing Knudsen diffusion. In this case, the measured self-diffusion coefficient D obtained by using the pulsed field gradient NMR method is given by the equation for the so-called fast-exchange limit

$$D = p_s D_s + p_g D_g \tag{8}$$

where p_s and p_g are the fractions (i.e., $p_g + p_s = 1$) of molecules in the adsorbed and the gaseous phase, respectively, with the corresponding diffusivities D_s and D_g.[28] Alternatively, the fractions p_i can also be represented as the relative lifetimes of the molecules in the corresponding phases. In our case, the applicability of eq 8 for description of the overall self-diffusion process is further related to the fact that molecular exchange between the phases may proceed in any point of the pore system, i.e., it is not diffusion-limited in either phase.[29,30]

In our recent paper,[17] we have shown that p_g and D_g can be well-represented by

$$p_g = \frac{1-\theta}{\theta}\frac{z(\theta)P_sM}{\rho RT} \tag{9a}$$

$$D_g = \frac{d\sqrt{1-\theta}}{3}\sqrt{\frac{8RT}{\pi M}} \tag{9b}$$

where M is the molar mass, R is the universal gas constant, T is the temperature, and ρ is the liquid density. In eq 9a, the fraction of molecules in the gaseous phase is explicitly related to the isotherm through $z(\theta)$, reflecting the fact of shifted equilibrium conditions between the adsorbed and the gaseous phases in pores with respect to bulk systems. In the gaseous phase, the molecular displacements are assumed to proceed via the Knudsen diffusion mechanism in a cylindrical pore with an effective pore diameter $d\sqrt{1-\theta}$. The term $\sqrt{1-\theta}$ in the last expression accounts for the reduction of the space available for the gaseous phase in a cylindrical pore due to the adsorbed phase.

For further consideration, it is more convenient to present the experimentally measured diffusivities in Figure 4b as a function of the concentration relying on the isotherms in Figure 4a. The result of such a transformation is shown in Figure 5 in a semilogarithmic plot. As well, shown is the course of p_gD_g calculated using eq 9 with the relevant physical properties of

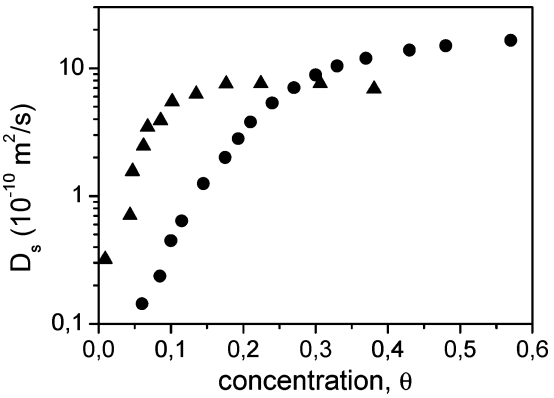

Figure 6. Surface diffusion coefficient D_s of cyclohexane (triangles) and acetone (circles) in porous silicon at partial pore loadings at $T = 297$ K.

the liquids under study at $T = 297$ K. It represents the contribution of the displacements through the gaseous phase to the total diffusivity D. With the data of Figure 5, the surface diffusion coefficient D_s can be obtained on the basis of the two-phase exchange model given by eq 8: $D_s = (D - p_g D_g)/(1 - p_g)$. Noting that $p_g \approx 10^{-4} \ll 1$, this relation is further simplified to $D_s \approx D - p_g D_g$. In Figure 6, we present the thus obtained data on D_s in the low-concentration region of interest. It is important to note that the term $p_g D_g$ is notably smaller than the measured diffusivity D at all concentrations (Figure 5). This means that the latter is only slightly altered by the Knudsen mechanism of diffusion. This is a direct consequence of the small pore size of about 3.6 nm. In our previous study,[17] we found that for pore sizes as big as 10 nm both mechanisms become equally important, i.e., give comparable contributions.

The most intriguing feature of the obtained data is a strong dependence of D_s on θ in the low-concentration region. A rough estimate of the concentration θ_s, corresponding to one-monolayer surface coverage in a cylindrical pore, is given by the relation $\theta_s \approx 4\sqrt[3]{v}/d$, where v is the effective volume of the molecules. With $\sqrt[3]{v} \approx 0.5$ nm, one finds $\theta_s \approx 0.5$. This estimate yields that the remarkably strong concentration dependence of D_s is observed at surface coverages smaller than one monolayer. Usually, such a phenomenon is attributed to surface diffusion on heterogeneous surfaces. This correlation shall be discussed in the following.

The often-used model of self-diffusion assumes random molecular jumps between nearest-neighbor sites with an average jump rate of the Arrhenius form.[5] Thus, the experimentally measured self-diffusion coefficients are usually analyzed using the equation

$$D = D_0 \exp\{-E_D/RT\} \tag{10}$$

where E_D is the effective activation energy for self-diffusion and D_0 is the preexponential factor. If the time required for a single jump is negligibly small in comparison with the mean residence time τ_0 on the adsorption sites, then D_0 can be represented in the form $D_0 = r_0^2/4\tau_0$, where r_0 is a mean intersite distance. If the adsorption sites on the surface have different adsorption energies, characterized by some site-energy distribution function, then at partial surface coverages the molecules will tend to reside on energetically more favorable sites.[31,32] Therefore, an increase of the apparent E_D with decreasing surface coverage should be observed. To check this, we have performed self-diffusion measurements over a broad range of temperatures with porous silicon samples containing a certain

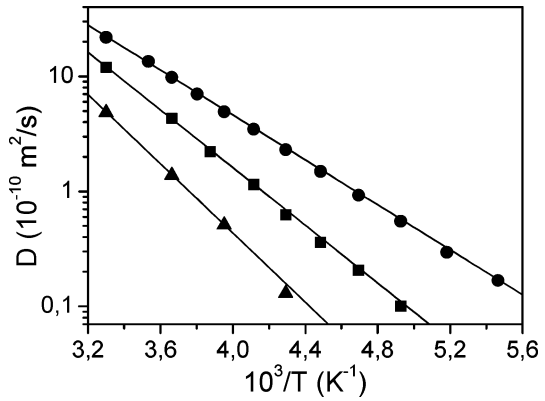

Figure 7. Dependence of the effective self-diffusion coefficient on temperature at different pore loadings $\theta = 0.6$ (circles), $\theta = 0.27$ (squares), and $\theta = 0.18$ (triangles). The solid lines show the best fits to the experimental data using eq 9 with the parameters given in Table 1.

TABLE 1: D_0 and E_D for Acetone in Porous Silicon at Different Concentrations θ Obtained by Fitting Eq 10 to the Experimental Data in Figure 7

θ	D_0, 10^{-5} m^2/s	E_D, kJ/mol
0.6	0.37	18.7
0.27	1.67	24.0
0.18	4.53	28.8

concentration of acetone molecules. To minimize a possible change of the intrapore concentration with variation of temperature, experiments were performed with the porous material placed in a 7 mm o.d. NMR tube with a length of about 6 cm, which thereafter was sealed upon saturating the sample to a required concentration. It is straightforward to show that the maximal possible change $\Delta\theta/\theta$ of the concentration in the pores attained upon transferring all of the molecules from the vapor phase in the NMR tube into the pores (e.g., by decreasing temperature) is

$$\frac{\Delta\theta}{\theta} = \frac{zP_sM}{\theta\rho RT}\frac{V_{tube}}{V_{pore}} \tag{11}$$

where V_{tube} and V_{pore} are the volume of the NMR tube and total pore volume, respectively. The calculations using corresponding parameters yield that $\Delta\theta/\theta$ is always less than 1%. Thus, we may claim that with a decrease in temperature the effects of vapor condensation into the pores are negligible.

Figure 7 shows the Arrhenius plots of the measured diffusivities. Most importantly, the plots are nearly linear over the temperature range investigated. The parameters D_0 and E_D obtained by fitting eq 10 to the experimental data are given in Table 1. The experimental finding of increasing E_D with decreasing concentration confirms the above conclusion on surface heterogeneity as deduced from the observed loading dependence.

The different shapes of the concentration dependencies of D_s for acetone and cyclohexane can be attributed to different affinities or interaction of these two species to the pore walls of the porous silicon. In fact, it is argued in the literature that the evidence provided by adsorption experiments on the surface characteristics may notably depend on the probe molecules.[3,33] This is also revealed by the particular details of the isotherms in Figure 4a. At very low concentrations, a step change is clearly observed for acetone, while it is less visible, if at all, for cyclohexane. Therefore, we may conclude that cyclohexane exhibits weaker adsorbate−adsorbent interaction than acetone.

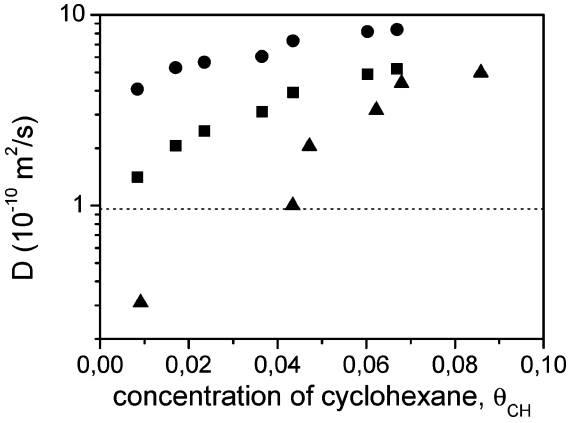

Figure 8. Measured self-diffusion coefficients of pure cyclohexane (D_{CH}, triangles, taken from Figure 5) and of a cyclohexane−acetone mixture (D_{tot}, rectangles) as well as the value of the partial diffusivity D_{CH} of cyclohexane in the cyclohexane−acetone mixture (filled circles) calculated using eq 12 as a function of the cyclohexane concentration θ_{CH} in the pores. The dotted line shows the diffusivity of the preadsorbed acetone with concentration $\theta_{AC} = 0.1$.

This may explain the nearly constant value of D_s for cyclohexane at concentrations above a certain critical value θ_{cr} of about 0.1. However, for $\theta < \theta_{cr}$, D_s again exhibits a strong dependence on θ. Such a behavior suggests that only a small part of the surface sites particularly strongly adsorb the cyclohexane molecules.

For further clarification, we performed the same type of experiments with binary mixtures adsorbed in the porous silicon. First, acetone was preadsorbed in order to yield the concentration $\theta_{AC} = \theta_{cr} = 0.1$. At this concentration, the self-diffusion coefficient of the acetone molecules is $D_{AC} = 0.96 \times 10^{-10}$ m^2/s. Thereafter, cyclohexane was added at a certain amount θ_{CH}, and the total diffusivity D_{tot} of the adsorbate molecules has been measured. Note that we could not distinguish between the cyclohexane and the acetone molecules due to insufficient resolution. At relatively low concentrations, when we can assume that the lateral adsorbate−adsorbate interaction is of minor influence, the measured diffusivity D_{tot} can be approximated by the equation

$$D_{tot} = p_{CH}D_{CH} + p_{AC}D_{AC} \qquad (12)$$

where p_{CH} and p_{AC} are the fractions of protons of the adsorbed cyclohexane and acetone molecules and D_{CH} and D_{AC} are their diffusivities. The fractions p_{CH} and p_{AC} are simply related to the respective concentrations, θ_{CH} and θ_{AC}.

In Figure 8, the measured diffusivities D_{tot} are shown as a function of the cyclohexane concentration θ_{CH}. With known concentrations, θ_{CH} and $\theta_{AC} = 0.1$, and with the reasonable assumption that D_{AC} does not appreciably change with changing the cyclohexane concentration, we can recalculate the partial diffusivity D_{CH} of cyclohexane using eq 12. This yields the diffusivities D_{CH} shown by the filled circles in Figure 8. As the most prominent feature of the obtained result, D_{CH} is found to be much faster than that for pure cyclohexane (shown by the triangles). Noting that θ_{AC} was chosen to be equal to θ_{cr}, we can speculate that the more strongly interacting acetone molecules occupy most of the surface sites responsible for the decrease in the diffusivity of the pure cyclohexane at $\theta < \theta_{cr}$. Thus, the diffusivity of the cyclohexane molecules in the mixture is mostly governed by random jumps among the less favorable surface sites, leading to their faster mobility. The fact that the absolute magnitudes of D_{CH} in the mixture are comparable with those for pure cyclohexane at $\theta > \theta_{cr}$ is in complete agreement with this conclusion.

Conclusions

We have presented an experimental study of the self-diffusion process of the organic molecules cyclohexane and acetone, physisorbed in porous silicon at different pore concentrations, using the pulsed field gradient NMR method. Due to the small size of the pores (∼3.6 nm), the concentration region corresponding to less than monolayer coverage has been well-captured. The contribution of the Knudsen mechanism to the measured diffusivities at partial pore loadings has been estimated and taken into account in the frame of a model proposed in ref 17. It allowed us to separate the surface diffusion coefficient from the experimental results. Importantly, the analysis performed yielded that surface diffusion (i.e., diffusion within the surface layer) is by far the dominant mechanism contributing to the measured diffusivities. Thus, the experimentally measured diffusivities are only slightly altered by the Knudsen mechanism of mass transfer through the gaseous phase, which is primarily a consequence of the small size of the pores (∼3.6 nm). This convinces us that the pulsed field gradient NMR method can be used to directly probe surface diffusion.

The surface diffusivities were found to exhibit a strong dependence on the concentration at surface coverages less than one monolayer. This fact is attributed to the heterogeneity of the surface, namely, the existence of a distribution of adsorptive energies. This can be primarily caused by a specific arrangement of the surface Si atoms in small pores and/or structural defects on the surface. The site-energy disorder leads to a preferential occupation of the energetically more favorable sites on the substrate at low surface coverages. Because the binding energy also determines the mean residence time, the resulting asymmetric occupation is shown to give rise to the observed behavior of the surface diffusivity. This picture is further confirmed by the experimentally obtained decrease of the apparent activation energy of diffusion with increasing surface coverage.

The concentration dependence of the diffusivities for acetone and cyclohexane was found to correlate with the adsorption properties. From the analysis of the isotherm shapes, it follows that acetone is subject to a stronger affinity to the surface than cyclohexane. This has to lead to a strong dependence of the surface self-diffusion coefficient of acetone on concentration in the whole range of surface coverage. At the same time, for the weaker interacting cyclohexane such a dependence is only observed at sufficiently low surface coverages. We may conclude, therefore, that only a part of the surface sites responsible for the relatively strong adsorption of the acetone molecules exhibits a similar affinity to the cyclohexane molecules. This conclusion is confirmed by investigating the effect of preadsorption of a certain amount of acetone molecules required to occupy such surface sites. In the presence of acetone molecules, the cyclohexane diffusivities are found to depend more weakly on concentration, with magnitudes notably exceeding those for pure cyclohexane. We anticipate that the surface heterogeneity caused by the existence of defects in the silicon pore walls with selective affinities to different molecules is responsible for the observed patterns of surface diffusion.

Acknowledgment. R.V. and V.T. thank the Alexander von Humboldt Foundation for financial support. We also thank Professor D. Ruthven for valuable discussions and an anonymous reviewer for helpful comments.

References and Notes

(1) Rudzinski, W.; Everett, D. H. *Adsorption of Gases on Heterogeneous Surfaces*; Academic Press: New York, 1992.

(2) Steele, W. A. *The Interaction of Gases with Solid Surfaces*; Pergamon: New York, 1974.

(3) Riccardo, J. L.; Chade, M. A.; Pereyra, V. D.; Zgrablich, G. *Langmuir* **1992**, *8*, 1518.

(4) Gomer, R. *Rep. Prog. Phys.* **1990**, *53*, 917.

(5) Barth, J. V. *Surf. Sci. Rep.* **2000**, *40*, 75.

(6) Choi, J. G.; Do, D. D.; Do, H. D. *Ind. Eng. Chem. Res.* **2001**, *40*, 4005.

(7) Antczak, G.; Ehrlich, G. *Phys. Rev. Lett.* **2004**, *92*, 166105.

(8) Briner, B. G.; Doering, M.; Rust, H. P.; Bradshaw, A. M. *Science* **1997**, *278*, 257.

(9) Mitsui, T.; Rose, M. K.; Fomin, E.; Ogletree, D. F.; Salmeron, M. *Science* **2002**, *297*, 1850.

(10) Callaghan, P. T. *Principles of Nuclear Magnetic Resonance Microscopy*; Clarendon Press: Oxford, 1991.

(11) Kärger, J.; Ruthven, D. M. *Diffusion in Zeolites and Other Microporous Solids*; Wiley & Sons: New York, 1992.

(12) Stallmach, F.; Karger, J. *Adsorption* **1999**, *5*, 117.

(13) Allen, S. G.; Mallett, M. J. D.; Strange, J. H. *J. Chem. Phys.* **2001**, *114*, 3258.

(14) D'Orazio, F.; Bhattacharja, S.; Halperin, W. P.; Eguchi, K.; Mizusaki, T. *Phys. Rev. B* **1990**, *42*, 9810.

(15) Dvoyashkin, N. K.; Skirda, V. D.; Maklakov, A. I.; Belousova, M. V.; Valiullin, R. *Appl. Magn. Reson.* **1991**, *2*, 83.

(16) Ardelean, I.; Mattea, C.; Farrher, G.; Wonorahardjo, S.; Kimmich, R. *J. Chem. Phys.* **2003**, *119*, 10358.

(17) Valiullin, R.; Kortunov, P.; Karger, J.; Timoshenko, V. *J. Chem. Phys.* **2004**, *120*, 11804.

(18) Stapf, S.; Kimmich, R. *Chem. Phys. Lett.* **1997**, *275*, 261.

(19) Lehmann, V.; Stengl, R.; Luigart, A. *Mater. Sci. Eng., B* **2000**, *69*, 11.

(20) Herino, R.; Bomchil, G.; Barla, K.; Bertrand, C.; Ginoux, J. L. *J. Electrochem. Soc.* **1987**, *134*, 1994.

(21) Coasne, B.; Grosman, A.; Dupont-Pavlovsky, N.; Ortega, C.; Simon, M. *Phys. Chem. Chem. Phys.* **2001**, *3*, 1196.

(22) Coasne, B.; Grosman, A.; Ortega, C.; Simon, M. *Phys. Rev. Lett.* **2002**, *88*, 256102.

(23) Strange, J. H.; Rahman, M.; Smith, E. G. *Phys. Rev. Lett.* **1993**, *71*, 3589.

(24) Sliwinska-Bartkowiak, M.; Gras, J.; Sikorski, R.; Radhakrishnan, R.; Gelb, L.; Gubbins, K. E. *Langmuir* **1999**, *15*, 6060.

(25) Cotts, R. M.; Hoch, M. J. R.; Sun, T.; Markert, J. T. *J. Magn. Reson.* **1989**, *83*, 252.

(26) Wu, D. H.; Chen, A. D.; Johnson, C. S. *J. Magn. Reson. A* **1995**, *115*, 260.

(27) Sorland, G. H.; Aksnes, D. *Magn. Reson. Chem.* **2002**, *40*, S139.

(28) Kärger, J.; Pfeifer, H.; Heink, W. *Adv. Magn. Reson.* **1988**, *12*, 2.

(29) Valiullin, R. R.; Skirda, V. D.; Stapf, S.; Kimmich, R. *Phys. Rev. E* **1997**, *55*, 2664.

(30) Kärger, J. *Adv. Colloid Interface Sci.* **1985**, *23*, 129.

(31) Kehr, K. W.; Mussawisade, K.; Wichmann, T. Diffusion of Particles on Lattices. In *Diffusion in Condensed Matter*; Kärger, J., Heitjans, P., Haberlandt, R., Eds.; Friedr. Vieweg & Sohn: Braunschweig/Wiesbaden, 1998.

(32) Cameron, L. M.; Sholl, C. A. *J. Phys.: Condes. Matter* **1999**, *11*, 4491.

(33) Marczewski, A. W.; Derylomarczewska, A.; Jaroniec, M. *J. Colloid Interface Sci.* **1986**, *109*, 310.